Balitskiĭ-Fadin-Kuraev-Lipatov equation versus data from DESY HERA

I. Bojak and M. Ernst
Institut für Physik, Universität Dortmund, D-44221 Dortmund, Germany
(Received 17 August 1995)

The BFKL equation and the k_T-factorization theorem are used to obtain predictions for F_2 in the small Bjørken-x region over a wide range of Q^2. The dependence on the parameters, especially on those concerning the infrared region, is discussed. After a background fit to recent experimental data obtained at DESY HERA and at Fermilab (E665 experiment) we find that the predicted, almost Q^2 independent BFKL slope $\lambda \gtrsim 0.5$ appears to be too steep at lower Q^2 values. Thus there seems to be a chance that future HERA data can distinguish between pure BFKL and conventional field theoretic renormalization group approaches.

PACS number(s): 13.60.Hb, 12.38.Bx, 12.38.Qk

I. INTRODUCTION

The usual kinematic variables used for discussing deep-inelastic electron-proton scattering are derived from the four-momenta p of the incoming proton and q of the exchanged virtual photon: $Q^2 \equiv -q^2$ and the Bjørken variable $x \equiv Q^2/2p \cdot q$. In the region where higher-twist effects are likely to be negligible, i.e., for $W^2 \equiv Q^2(1/x - 1) \gtrsim 10$ GeV^2, the (Dokshitzer-Gribov-Lipatov-)Altarelli-Parisi [(DGL)AP] set of equations [1,2] describes the evolution of the structure function F_2 with Q^2 very well. In leading order (LO) all powers of $\alpha_s \ln(Q^2/\mu^2)$ are summed by the AP evolution equations, which take into account just strongly ordered parton-k_T ladders. Nowadays, usually, the next-to-leading order (NLO) set is used, where terms of the form $\alpha_s^n \ln^{n-1}(Q^2/\mu^2)$ are also summed, taking *nonordered* k_T contributions (covariantly) into account as well. Even in NLO, the AP equations do obviously not contain all leading logarithms in x. Thus one might naively expect the AP framework to break down at some small value of x, where a resummation of all powers of $\alpha_s \ln(1/x)$ should be necessary, although no perturbative instability between LO and NLO has been observed thus far in the presently relevant kinematic regime [3–5].

Such a resummation in LO is provided by the Balitskiĭ-Fadin-Kuraev-Lipatov (BFKL) equation [6]. The equation treats the gluons only, which are expected to be the dominant partons at small x. This might be deduced from the AP splitting functions [1], which become $\sim 1/x$ for splitting to gluons and constant for splitting to quarks in the small-x limit. It should be remarked, though, that this argument may be too simple, as it neglects the influence of the particular shape of the parton distributions used [4,5] and furthermore does not respect the fundamental energy-momentum conservation constraint. The BFKL resummation is formally correct for all Q^2, but a fixed coupling $\bar{\alpha}_s$ was used in its derivation. Furthermore, it was based on LO perturbation QCD, using (noncovariant) k_T cutoff regularizations; thus, we are limited to sufficiently large Q^2. Since the resummation assumes that subleading terms in x are small, including those involving logarithms of Q^2, it will also not be valid at high Q^2. A conservative range for Q^2 would be 4–50 GeV^2, and the range 0.8–120 GeV^2 explored in this work should be regarded as the extreme limit.

To estimate the effects of the subleading terms, a NLO resummation in x would be necessary. But even though there has been some progress in that direction [7], a final result has not yet been obtained. Ultimately, it should even be possible to find a unified evolution equation covering the whole perturbative region [8–10]. But a calculation that can be confronted with experiment is still missing; thus, we stay with the usual BFKL formalism for the time being.

Since a fixed coupling constant seems unreasonable in view of the running coupling of the AP framework we wish to connect to, the replacement $\bar{\alpha}_s \to \alpha_s(Q^2)$ is done by hand. There is really no rigorous motivation for this step. Some trust in this procedure can be gained by considering the representation of the evolution equations as ladder diagrams. It is well known that the LO AP equations can be represented in a physical gauge by a sum of ladder graphs which are strongly ordered in the transverse momentum k^2: $Q^2 \gg k^2 \gg k_{n-1}^2 \gg \cdots k_1^2 \gg k_0^2$. In the small-$x$ limit of the AP equation, we consider only the dominant gluon ladder (Fig. 1) and keep only the terms with double leading logarithms (DLL's), $\alpha_s \ln(1/x) \ln(Q^2/\mu^2)$. This corresponds to introducing an additional strong ordering in x: $x \ll x_{n-1} \ll \cdots \ll x_0$. The BFKL evolution can also be described in terms of a (Reggeized) gluon ladder, using the strong ordering in x only, to get the leading logarithms in x. If we let the coupling run, then the BFKL evolution will reduce to LO DLL's upon imposing the strong ordering in transverse momentum.

The main feature of the BFKL evolution with fixed coupling $\bar{\alpha}_s$ is the growth of the unintegrated gluon $\sim x^{-\lambda}$ with $\lambda = (3\bar{\alpha}_s/\pi)4\ln 2 \simeq 0.5$. Because of the dominance of the gluons at small x, we expect a corresponding rise at small x in the structure functions too, once the off-shell gluons have been appropriately coupled to the quark sector. This expectation has been confirmed [11,12] for a small range of medium Q^2 even in the case

 ©1996 The American Physical Society

of running coupling BFKL evolution, with $F_2 \sim x^{-\lambda}$ and $\lambda \gtrsim 0.5$ for $x < 10^{-3}$.

Experimentally, the situation has improved drastically since the advent of the DESY *ep* collider HERA. Before HERA only the Fermilab experiment E665 [13] was able to reach the small-x region, but at rather low Q^2. Now HERA takes data [14,15] with $x/Q^2 \gtrsim 3 \times 10^{-5}$ over a wide range of Q^2. The observed strong rise of F_2 at small x has boosted the interest in the BFKL formalism. On the other hand, the dynamically generated AP partons [5] create a steep gluon differently, via a long evolution length in Q^2, and successful parameter-free predictions [3,5,16] were given long before HERA started to operate. Alternatively, the present data can be fitted using the NLO AP evolution equations: Then a term $\sim x^{-\lambda}$ has to be *assumed* for the gluon distribution, e.g., in Martin-Roberts-Stirling set G (MRSG) [17]. Possibly this term mimicks the BFKL behavior. But this is not clear, since both methods describe the data equally well.

We conclude that a detailed comparison of the standard BFKL formalism with the new data is necessary. Only this can tell us if the BFKL formalism can rival conventional field theoretic renormalization group (AP) evolution equations in describing the measured structure function F_2. Our calculations are based on the methods employed by Askew, Kwieciński, Martin, and Sutton (AKMS) [11,12,18], which will be described briefly in the following.

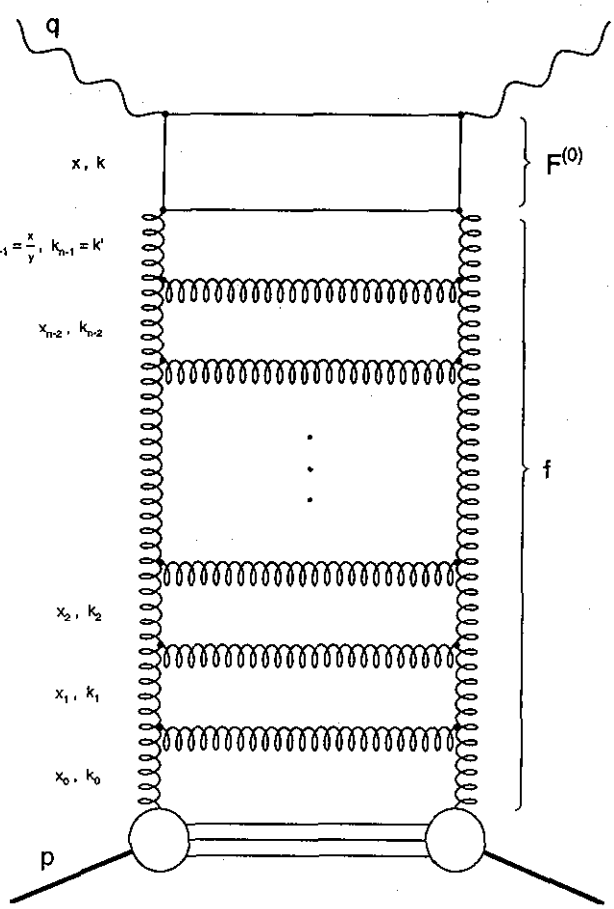

FIG. 1. Gluon ladder with the quark box for deep-inelastic *ep* scattering attached. The momenta are shown on the left side of the Feynman diagram and the parts of the k_T-factorization theorem, Eq. (3), on the right.

A. BFKL equation and k_T factorization

The unintegrated gluon distribution $f(x,k^2)$, which is related to the familiar integrated gluon distribution used in the AP equations by

$$xg(x,Q^2) = \int_0^{Q^2} \frac{dk^2}{k^2} f(x,k^2) \ , \tag{1a}$$

$$f(x,k^2) = \left. \frac{\partial x\, g(x,Q^2)}{\partial \ln(Q^2)} \right|_{Q^2=k^2} , \tag{1b}$$

depends on the transverse momentum k. Using it, one can write the BFKL equation as [19]

$$f(x,k^2) = f_0(x,k^2) + \int_x^1 \frac{dy}{y} \int dk'^2 K(k^2,k'^2) f(y,k'^2)$$

$$K(k^2,k'^2) = \frac{3\alpha_s(k^2)}{\pi} k^2 \left\{ \frac{1}{k'^2|k^2-k'^2|} - \beta(k^2)\delta(k^2-k'^2) \right\} ,$$

$$\beta(k^2) = \int \frac{dk'^2}{k'^2} \left\{ \frac{1}{|k^2-k'^2|} - \frac{1}{(4k'^4+k^4)^{\frac{1}{2}}} \right\} .$$

One could use a suitable input f_0, the so-called "driving term," and solve the equation iteratively [10], but this procedure allows no simple connection to the known AP region.

Instead we can obtain an evolution equation in x from the integral equation by differentiating with respect to $\ln(1/x)$:

$$-x\frac{\partial f(x,k^2)}{\partial x} = \frac{3\alpha_s(k^2)}{\pi} k^2 \int \frac{dk'^2}{k'^2} \left[\frac{f(x,k'^2)-f(x,k^2)}{|k'^2-k^2|} + \frac{f(x,k^2)}{(4k'^4+k^4)^{1/2}} \right] , \tag{2}$$

assuming that the derivative of the driving term f_0 can be neglected. Since the driving term describes the gluon content without any BFKL evolution, it is reasonable to assume that it is connected to the nonperturbative "soft" Pomeron [20]. Because of the soft Pomeron's weak x dependence $\sim x^{-0.08}$, we expect $\partial f_0/\partial \ln(1/x)$ to be small.

Equation (2) can then be used to evolve the unintegrated gluon to smaller x, using a suitably modified AP input as boundary condition at $x_0 = 10^{-2}$ by applying Eq. (1b). An obvious problem in Eq. (2) is posed by the integration over k'^2, which starts at zero. Even for the AP gluon distributions we use in this work, the limit of validity is about 1 GeV^2. We employ a simple ansatz to continue the gluon into the infrared (IR) region, which

will be described later in this paper. A similar comment applies to the upper limit of the k'^2 integration. The upper limit introduced by energy conservation is close to infinity [11,12], so that for practical calculations an artificial ultraviolet cutoff has to be introduced. The dependence on the IR and UV treatment will be thoroughly discussed later on.

To obtain predictions for F_2, we have to convolute the (off-shell) BFKL gluon, i.e., the gluon ladder in Fig. 1, with a photon-gluon fusion quark box $F^{(0)}$ using the k_T-factorization theorem [9,21]

$$F_i(x,Q^2) = \int \frac{dk'^2}{k'^4} \int_x^1 \frac{dy}{y} f\left(\frac{x}{y}, k'^2\right) \times F_i^{(0)}(y, k'^2, Q^2) \ , \tag{3}$$

with $i = T$ and L denoting the transverse and longitudinal parts, respectively. The expressions for $F^{(0)}$ can be found in [18] and references therein. The BFKL prediction for F_2 is then simply the sum of the calculated F_T and F_L. Obviously, here the same problems with the k'^2 integration occur, which are circumvented by the methods mentioned above.

It is important to notice that the BFKL gluons are *off shell* ($k^2 \neq 0$). The term $F^{(0)}/k^2$ in the above equation then corresponds to the structure function of a virtual gluon. In contrast, the AP formalism is based on *on-shell* gluons, which is a good approximation due to the strong ordering in transverse momentum encountered in the AP evolution in LO. This strong ordering allows us to perform the k'^2 integration in Eq. (3). Thus, ignoring complications due to the collinear singularities for simplicity, one arrives at the usual mass factorization equation

$$F_i(x,Q^2) = \int_x^1 \frac{dy}{y} g\left(\frac{x}{y}, Q^2\right) \hat{F}_i(y,Q^2) \ .$$

Here $\hat{F}_i$ plays the role of the on-shell gluon structure function, whose x dependence stems from the AP splitting function P_{qg} and g is the integrated gluon. In the NLO AP evolution, the strong ordering in k^2 does not hold anymore due to the emission of a second gluon, but the interacting gluon is still considered to be on shell in comparison with the hard scattering scale Q^2.

This shows that it is inconsistent to simply feed the evolved BFKL gluon via Eq. (1a) back into the AP equations below the limit set by x_0. Calculations attempting to use BFKL gluons below and AP gluons above x_0 within the AP formalism [22] ignore the essential *off shellness* of the BFKL gluons. This casts first doubts on a recent BFKL analysis of the HERA H1 data using this method [23]. No such problem persists when we use just this gluon mixture to drive the general k_T factorization, Eq. (3), which reduces to the mass factorization in the AP region.

Even though the dominant contribution at small x should come from the BFKL gluons, a certain amount of "background" in F_2 due to quarks and nonperturbative effects should be taken into account. We expect the background to be comparatively small and also to vary much less with x. We shall use an ansatz motivated by the soft Pomeron $C_{\mathbb{P}} x^{-0.08}$, where the constant $C_{\mathbb{P}}$ is fitted to the data. After this general outline of our method, we will now proceed to a detailed discussion of the underlying formalism.

II. SUITABLE INPUT FOR THE BFKL EVOLUTION

We focus our analysis on the gluon distribution used in [12], i.e., a gluon based on the MRS D_0 set of parton distributions [24], but evolved with the leading order Altarelli-Parisi equations [25]. Since the BFKL evolution deals with an *unintegrated* gluon distribution, we calculate its derivative using the well-known singlet Altarelli-Parisi equation given by

$$f^{\rm AP}(x,Q^2) = \frac{\alpha_s(Q^2)}{2\pi} \int_x^1 \frac{dy}{y} \left[P_{gg}^{(0)}\left(\frac{x}{y}\right) g(y,Q^2) + P_{gq}^{(0)}\left(\frac{x}{y}\right) \Sigma(y,Q^2) \right] ,$$

where Σ denotes the quark singlet part and $P_{gg}^{(0)}, P_{gq}^{(0)}$ the usual LO splitting functions. In the same way we produce a leading order MRS D_- type gluon, based on an input given in [26].

We also use a dynamically generated gluon distribution, for definiteness the Glück-Reya-Vogt (GRV) 1992 LO parametrization [3], which has the advantage of (a) being based on an explicit LO calculation and (b) being positive definite down to a low value of Q^2.

Furthermore, we take a look at the MRSA low-Q^2 gluon [27], which extends the valid Q^2 range down to 0.625 GeV^2, using an *ad hoc* form-factor-like ansatz similar to the one we employ for f. However, as MRSA is a NLO analysis, there is no consistent way to implement it in our BFKL evolution, which is neither a modified minimal subtraction ($\overline{\rm MS}$) nor deep inelastic scattering (DIS) renormalization scheme calculation.

A. Treatment of the infrared region

As mentioned in the Introduction, we need a suitable description of the infrared region; for our calculations, we use the ansatz explained in detail in [11,12]. This ansatz introduces three parameters.

(i) An IR "cutoff" k_c^2, i.e., a parameter which separates the infrared region, where an assumption on the k^2 behavior of f has to be made, from the region where the Lipatov equation is solved numerically.

(ii) A parameter k_a^2 that controls the infrared behavior of f. For $k^2 < k_c^2$ we set

$$f(x,k^2) = C' \frac{k^2}{k^2 + k_a^2} f(x,k_c^2) \ . \tag{4}$$

The proportionality constant is given by

$$C' = \frac{k_c^2 + k_a^2}{k_c^2} ,$$

to guarantee continuity at $k^2 = k_c^2$. This ansatz ensures that for $k^2 \to 0, f(x, k^2) \sim k^2$, as required by gauge invariance.

(iii) A scale k_b^2 where we "freeze" the running coupling constant: i.e.,

$$\alpha_s(k^2) \to \alpha_s(k^2 + k_b^2) .$$

This procedure applies also to our boundary condition $f(x_0, k^2)$, although there is a slight modification to the pure AP gluon in order to soften its low-k^2 behavior:

$$f^{\rm AP}(x_0, k^2) \to f^{\rm AP}(x_0, k^2 + k_s^2) . \tag{5}$$

The only purpose of the additional parameter k_s^2 is to ensure that we do not approach too closely a region where the gluon is unreliable; e.g., the D_0-type gluon already approaches zero at $Q^2 = 1$ GeV^2 and the D_--type gluon is not defined at all for such a low scale.

Thus

$$f(x_0, k^2) = \begin{cases} \frac{k^2}{k^2+k_a^2} f^{\rm AP}(x_0, k_c^2 + k_s^2) & \text{for } k^2 < k_c^2 , \\ \frac{k^2}{k^2+k_a^2} f^{\rm AP}(x_0, k^2 + k_s^2) & \text{for } k^2 \geq k_c^2 . \end{cases} \tag{6}$$

This provides an infrared behavior according to (4) and for k^2 large enough $f(x_0, k^2)$ approaches $f^{\rm AP}(x_0, k^2)$.

In Ref. [11], the parameter k_s^2 is set equal to k_a^2, whereas in [12] k_s^2 equals k_b^2. We prefer setting $k_s^2 = k_a^2$ for reasons given below.

B. Fixing k_a^2

It seems to be clear that the parameters introduced above should be small; so the simplest choice for these would be [12]

$$k_a^2 = k_b^2 = k_c^2 = k_s^2 = 1 \text{ GeV}^2 . \tag{7}$$

However, there is a self-consistency constraint on the choice of k_a^2, depending on k_c^2 and x_0. The boundary condition (6) should inversely be related to the (integrated) Altarelli-Parisi gluon g in Eq. (1a), that is,

$$x_0 g(x_0, Q^2) - \int_0^{Q^2} \frac{dk^2}{k^2} f(x_0, k^2) = 0 . \tag{8}$$

In a stricter approach, we apply the shift introduced in (5) also to the integrated gluon g in this equation. Then it is not very difficult to show that

$$\int_{k_c^2+k_a^2}^{Q^2+k_a^2} dl^2 \left(1 + \frac{k_s^2 - k_a^2}{l^2}\right) \frac{\partial x_0 g(x_0, Q^2)}{\partial Q^2}\bigg|_{Q^2 = l^2 + k_s^2 - k_a^2} = x_0 g(x_0, Q^2 + k_s^2) - x_0 g(x_0, k_c^2 + k_s^2) . \tag{9}$$

It is obvious that this equation is satisfied by setting $k_s^2 = k_a^2$, hence motivating our previous assumption. Using this and the asymptotic behavior of g,

$$x g(x, Q^2 + k_s^2) \overset{Q^2 \gg k_s^2}{\simeq} x g(x, Q^2) , \tag{10}$$

we may return to (8) for simplicity, which gives us, upon inserting our boundary condition (6),

$$\begin{aligned} x_0 g(x_0, Q^2) &= \int_0^{k_c^2} \frac{dk^2}{k^2 + k_a^2} f^{\rm AP}(x_0, k_c^2 + k_a^2) + \int_{k_c^2}^{Q^2} \frac{dk^2}{k^2 + k_a^2} f^{\rm AP}(x_0, k^2 + k_a^2) \\ &\simeq f^{\rm AP}(x_0, k_c^2 + k_a^2) \ln \frac{k_c^2 + k_a^2}{k_a^2} + x_0 g(x_0, Q^2) - x_0 g(x_0, k_c^2 + k_a^2) . \end{aligned}$$

Thus we obtain an implicit equation for k_a^2:

$$\ln \frac{k_c^2 + k_a^2}{k_a^2} \simeq \frac{x_0 g(x_0, k_c^2 + k_a^2)}{f^{\rm AP}(x_0, k_c^2 + k_a^2)} . \tag{11}$$

One can see that the value of k_a^2 mainly depends on the ratio g/f in the region of low Q^2, and as the variation of f for different parton distributions is relatively small in that region compared to the variation of g, we conclude that it is basically the absolute value of g that determines the size of k_a^2. Hence, as a rule of thumb, the higher the value of $x_0 g(x_0, Q^2)$ for small Q^2, the smaller the resulting k_a^2. It should be emphasized that, although the shift in Eq. (5) is taken into account in Eq. (9) for both f and g, but in Eq. (11) only for f, the solution of Eq. (11) provides a good estimate on k_a^2, very close to the value we get by minimizing the left-hand side of Eq. (8) for $Q^2 > 100$ GeV^2. The result for all the parton distributions under consideration is given in Table I, together with the value of $\Lambda_{\rm QCD}$ for four flavors used with each distribution. Figure 2 shows the unmodified gluons and the modified boundary conditions according to Table I.

Regarding the D_0-type gluon, we see that the optimized value of $k_a^2 = 0.95$ GeV^2 is indeed very close to the naive estimate of 1 GeV^2, as was already noticed in [12]. It was also mentioned there that a reasonable choice of k_a^2 should lie in the range of 0.5–2 GeV^2, and

TABLE I. Parameters for various sets of parton distributions.

Set	$\Lambda^{(4)}_{\rm QCD}$ (MeV)	x_0	k_c^2 (GeV^2)	k_a^2 (GeV^2)
D_0-type	173.2	0.01	1.0	0.95
D_--type	230.4	0.01	1.0	1.51
GRV 1992-LO	200.0	0.01	1.0	0.19
MRSA low Q^2	230.2 ($\overline{\rm MS}$)	0.01	1.0	0.44

we see that the D_--type value lies well within this range, while the MRSA set is already close to its lower edge. The most extreme boundary condition in this respect is derived from the GRV parametrization, with a value of only 0.19 GeV^2.

As the more recent parton distributions favor a larger gluon g, the assumption of $k_a^2 = 1$ GeV^2 (a good choice for the relatively small D_0-type gluon) does not appear to be the best choice for these gluons.

Let us now emphasize the importance of the constraint (8) on k_a^2: Starting with the simple assumption (7) that all the parameters introduced should be equal to 1 GeV^2, one gets a slope

$$\lambda = \frac{1}{f}\frac{\partial f}{\partial \ln(1/x)}\bigg|_{x=10^{-4}} = 0.5\text{–}0.6 \qquad (12)$$

for the unintegrated BFKL-evolved gluon distribution, as expected, no matter if D_0-type, D_--type, or GRV is chosen as input for the BFKL evolution. If we deviate each of the infrared parameters from (7), we see that it is k_a^2 which has the biggest impact on λ. With k_a^2 decreasing, the slope rises, resulting in a slope $\lambda \simeq 0.9$ for GRV partons ($k_a^2 = 0.19$ GeV^2) as the extreme limit.

Keeping these considerations in mind, we will now concentrate our analysis on the structure functions. We will demonstrate that the slopes of f and F_2 are related in such a way that for large λ our calculated F_2 is too steep to match it to the recent HERA data.

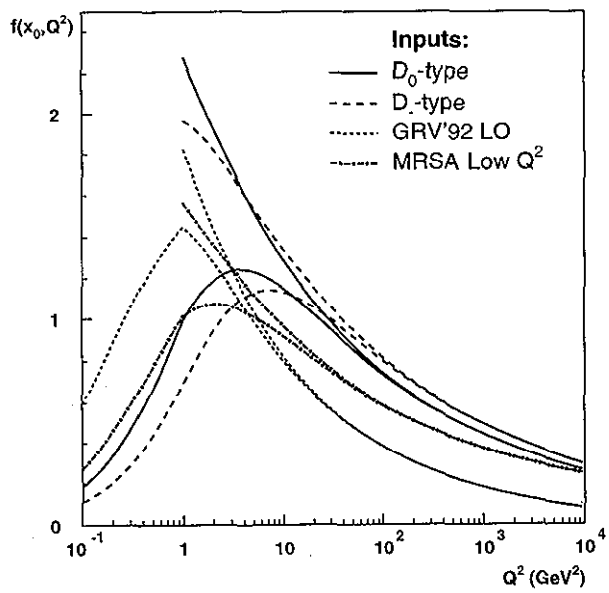

FIG. 2. AP inputs as indicated and the corresponding boundary conditions constructed via Eq. (6). The unmodified AP gluons are shown down to $k_c^2 = 1$ GeV^2, whereas the IR-treated inputs are continued below k_c^2.

III. VARYING THE PARAMETERS

We construct the boundary condition at $x_0 = 10^{-2}$. The consistency constraint (8) determines k_a^2, and as a standard value for the other two IR parameters we choose $k_b^2 = k_c^2 = 1$ GeV^2. The UV cutoff is set to 10^4 GeV^2 and we stay with the $\Lambda_{\rm QCD}$ of the AP partons. We have written an evolution program to solve (2) iteratively. Below k_c^2 the necessary integration can easily be done analytically; above, we use the Gauss-Legendre quadrature. This transforms the integro-differential equation (2) into a set of coupled differential equations, allowing us to use the standard Runge-Kutta method to calculate the evolution. The evolved gluon below x_0 is combined with the unintegrated AP gluon above x_0 to obtain predictions for F_T and F_L by performing the integration in Eq. (3) with Monte Carlo methods. For convenience, a fit of $F_2 = F_T + F_L$ is given in the Appendix. Finally, we fit the background to the data, as discussed at the end of Sec. I A, and obtain our BFKL prediction.

It is vital to check the dependence of the results on the parameters used for the IR and UV treatment. In Fig. 3 we varied all relevant parameters, using the D_0-type gluon. All curves have been calculated at $Q^2 = 15$ GeV^2

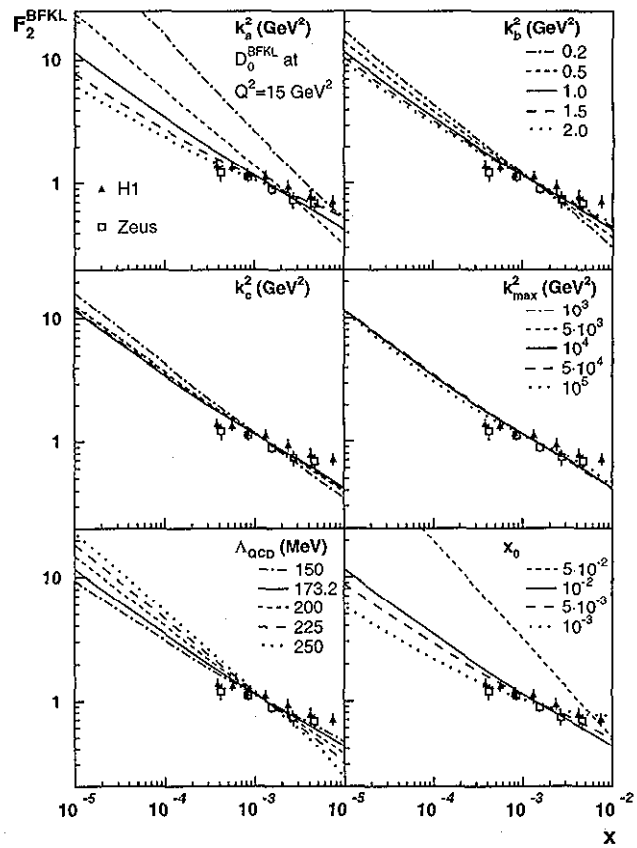

FIG. 3. Variations of the parameters. All curves are calculated at $Q^2 = 15$ GeV^2 with the D_0-type gluon input. The background $C_{\mathbb{P}}x^{-0.08}$ has already been added to the BFKL curves, and statistical and systematic errors of the data have been added in quadrature in this and all following figures. The legend for k_b^2 is the same also for k_a^2 and k_c^2.

and are already fitted to the shown HERA data with the soft Pomeron background $C_{\mathbb{P}} x^{-0.08}$.

The strong dependence on k_a^2, which we expect from the corresponding variation in the gluon slope, is obvious. The curves for low k_a^2 are much too steep. At $k_a^2 = 0.2$ GeV^2, for example, the pure BFKL prediction is too high, even without any background. A background fit would then give a *negative* contribution, i.e., $C_{\mathbb{P}} < 0$, which is unphysical. In all such cases, we set the background to zero. It is crucial that k_a^2 can be precisely determined from the consistency constraint. Without the constraint, we could vary the slope of F_2 from 0.5 to 0.8 by choosing k_a^2 within the shown range of 0.2–2.0 GeV^2, rendering any serious prediction impossible. In the already mentioned comparison of a BFKL calculation with HERA data [23], k_a^2 is treated as a *free* parameter. If the fitted k_a^2 should not be close to the consistent value by chance, it is doubtful that any strong conclusions can be drawn from a successful description of the data.

The influence of the IR cutoff k_c^2 is comparably small. It should be kept in mind that k_a^2 has to be fitted separately for each k_c^2. Actually, the induced variations in k_a^2 dampen the dependence of the predictions on k_c^2 slightly. It is no surprise that variations of the UV cutoff do not introduce much uncertainty into the predictions, as the running coupling already serves as an effective UV cutoff [11,12]. The remaining free IR parameter k_b^2 has a sizable effect on the curves. The slope of F_2 varies from 0.53 to 0.58 in the shown k_b^2 range. The standard value of 1 GeV^2 gives a slope of about 0.55, and the variations of k_b^2 represent an effective error band of our calculations.

A considerable dependence on $\Lambda_{\rm QCD}$ is expected and can be seen in Fig. 3. Fortunately, this parameter is fixed, since we are using AP gluons with a given $\Lambda_{\rm QCD}$ as the boundary condition. It is interesting to note that higher values of $\Lambda_{\rm QCD}$ than the rather low 173.2 MeV used in the D_0-type partons give *unfavorably* steep slopes. Finally, we take a look at variations of x_0, noting that we have to determine k_a^2 separately again. We expect the steep curve for $x_0 = 5 \times 10^{-2}$ due to the long evolution length in x. But it is daring to use the BFKL equations at such high values of x and the data do not support such a choice. We can also see that the comparably flat curve created by a short evolution in x starting from $x_0 = 10^{-3}$ does fit the data well. But this success can obviously not be claimed by the BFKL evolution, since the data do not extend far below that x_0. In order to test if the BFKL equations can describe the *current* data, we have to choose a larger $x_0 \sim 10^{-2}$. The typical steep BFKL slope simply needs enough evolution length to develop. Small variations to lower x_0 from the usually used 10^{-2} do not affect the calculations strongly. The standard values [11,12] used for k_b^2 and x_0 give slopes slightly below and above the average expected from the variations, respectively. Thus this choice of parameters will give a sensible prediction while still allowing comparisons with earlier calculations [11,12].

The results presented in this section show that the dependence of the calculations on the parameters is under control. This statement would be impossible if k_a^2 did not obey the consistency constraint (8).

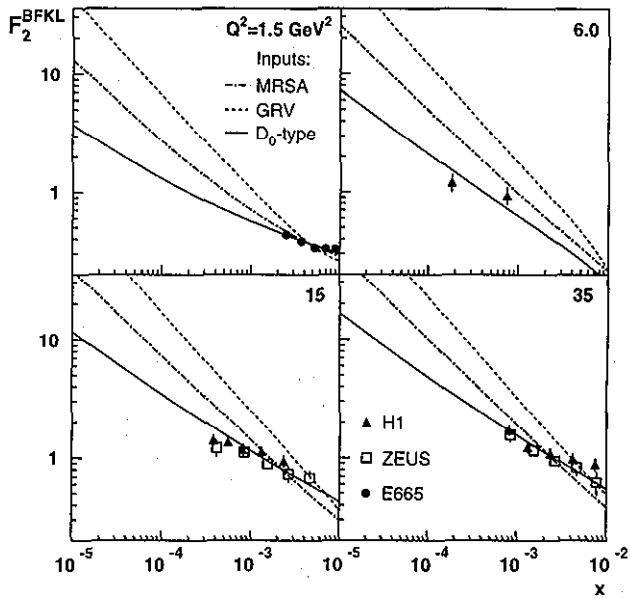

FIG. 4. Comparison of BFKL results, using MRSA low-Q^2 and GRV 1992 LO gluon inputs, compared with data at several Q^2. The corresponding curves for the D_0-type gluon input are shown for comparison.

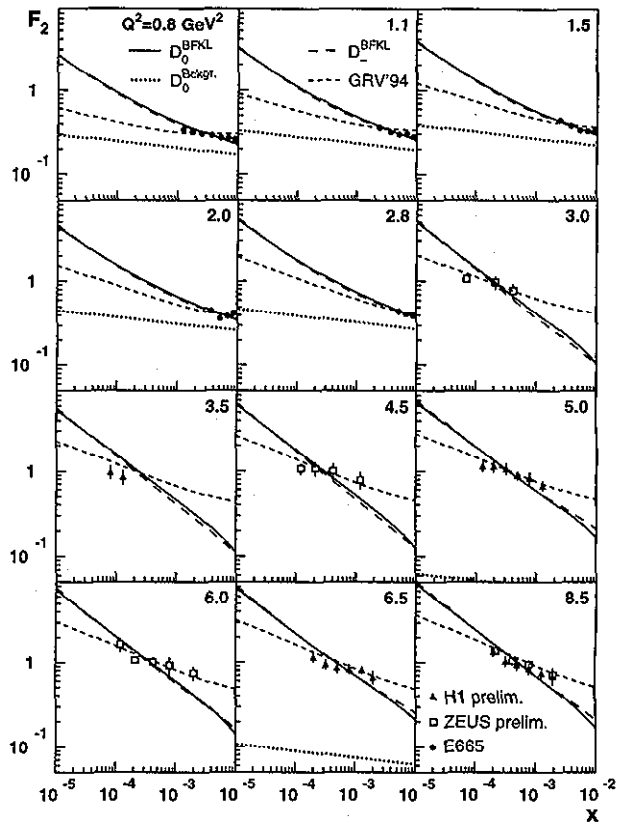

FIG. 5. Low-Q^2 data of the Fermilab E665 experiment [13] and preliminary data of the HERA experiment [15] in comparison with our BFKL results. The background included in the D_0-type curves is separately displayed. Note that "GRV '94" refers to the conventional dynamical results based on the NLO AP evolution of valencelike input parton densities [5].

A. Using other input distributions

Besides our detailed analysis of the D_0-type gluon, we also studied the effect of feeding different parton distributions into our evolution, namely, GRV 1992 LO [3] and MRSA low Q^2 [27]. The results for F_2 can be seen in Fig. 4.

Obviously, by using GRV and MRSA gluons as inputs for the BFKL evolution, a structure function is generated which is far too steep for the data. Even though we have got, in principle, some freedom in fitting an appropriate background, this is useless here, since already the pure BFKL part of F_2 is too high for the HERA data, so that we must set the background to zero.

The steepness of F_2 is closely related to the fact that the proper k_a^2 is much smaller than 1 GeV^2, resulting in a larger slope λ of the BFKL gluon f. As we explained above, this is mainly an effect of the size of the integrated gluon input g. This suggests the conclusion that the whole BFKL procedure has only a chance to work with the older (smaller) gluons. Modern parton distributions imply small values of the crucial infrared parameter k_a^2, and since this has a strong effect on the calculated structure functions, it is likely that one does not succeed in matching these to present experimental data.

IV. COMPARISON WITH DATA

In Fig. 5 we compare our calculations with very-low-Q^2 data from the Fermilab E665 experiment [13]. Preliminary data of the HERA ep collider [15] at low Q^2 are also shown in this figure. The published 1993 HERA data [14] for low to medium Q^2 are presented in Fig. 6 together with our BFKL predictions. All graphs show the BFKL calculations based on the D_0-type and D_--type partons, as well as the latest dynamical NLO renormalization group predictions (GRV), as presented in [5]. Also shown is the soft Pomeron background, which is included in the D_0-type curve. A general feature of all figures is that the difference between the D_0-type and D_--type BFKL predictions is very small after fitting the background. For this reason we do not discuss them separately. We have checked that the $R = F_L/F_T$ values used to extract F_2 from the experimental data are close enough to those predicted by BFKL. Thus it is not necessary to reanalyze the data in terms of $R_{\rm BFKL}$.

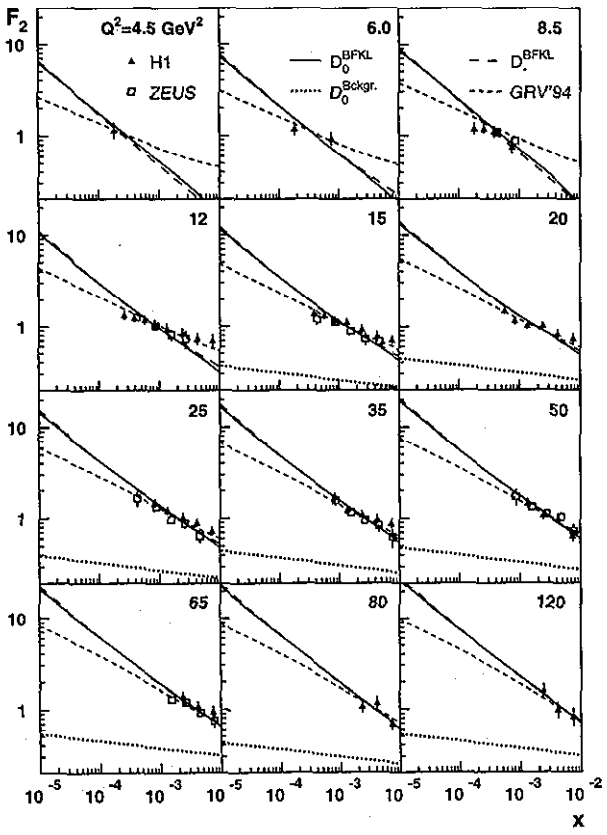

FIG. 6. As in Fig. 5, but using the HERA data of Ref. [14].

We first turn our attention to the E665 data [13]. The data do not extend very far into the small-x region, making a check of the BFKL behavior difficult. On the other hand, the difference between the GRV (AP) and BFKL predictions is potentially large at small x. We also notice that the added background is comparable in size to the BFKL part at higher x. This flattens the steep BFKL behavior, giving a good description of the data. But it is just the large contribution of the background which makes the very procedure used doubtful.

A further hint, that the successful description of the E665 data should not be taken too seriously, is provided by comparing the curves for the E665 data at 2.8 GeV^2 and those for preliminary ZEUS data at 3.0 GeV^2. While the E665 background is strong ($C_{\mathbb{P}} = 0.189$) for D_0 type, the optimal ZEUS background would be negative ($C_{\mathbb{P}} = -0.172$) and therefore is set to zero. Thus the natural requirement, that the BFKL predictions for similar Q^2 values should be approximately equal, is only fulfilled at very small x. For $x \gtrsim 10^{-4}$ the influence of the background quickly becomes stronger and the curves deviate. We conclude that BFKL *cannot* describe both data sets consistently. It is also obvious from the figures that just this is possible using the usual NLO renormalization group equations; see the curves labeled GRV '94 in Fig. 5.

Turning to the preliminary HERA data in Fig. 5, we find that the BFKL slope of F_2 is evidently too steep. The same tendency can also be found in the 1993 HERA data up to approximately 15 GeV^2 as shown in Fig. 6. Everywhere in this region the background is very small or would even be negative, if it were allowed. Because of the larger spread in x, the preliminary data show the discrepancy rather clearly. The problem is rooted in the almost Q^2-independent slope of BFKL, which is always $\gtrsim 0.5$ and grows weakly with Q^2. The dynamical GRV (AP) calculations give on the contrary flat slopes at low Q^2, which rise significantly with larger Q^2. This is obviously in much better agreement with the data. For example, using the preliminary ZEUS data at 4.5 GeV^2, we get a total χ^2 of 15.3 (D_0-type), 15.0 (D_--type), and 2.81 (GRV 1994 NLO) for the four data points.

At Q^2 higher than 15 GeV^2, we see that the slope of the data becomes compatible with the one predicted by BFKL. The rising slope of the dynamical GRV prediction fits the data at least as well. It is interesting to note that even at higher Q^2 a slight extension in the x range

could provide an indication which evolution should be used. If future data should conform to the already visible tendency that a Lipatov-like slope is only obtainable at high Q^2, say, $\gtrsim$ 50 GeV^2, then the simple LO BFKL formalism would become implausible, since its validity at such high Q^2 is questionable.

V. CONCLUSIONS

We have shown that the AKMS method for calculating BFKL predictions of F_2 remains stable under variations of the introduced parameters if the consistency constraint Eq. (8) on k_a^2 is applied. As boundary conditions, one has to choose older, i.e., smaller, gluon densities, since the large recent AP gluons lead to small k_a^2, which in turn produces overly steep slopes of F_2. The BFKL boost at small x is simply too large for gluons constructed to produce the measured large F_2 slope via the conventional renormalization group (AP) evolution equations.

Thus we use the old D_0-type and D_--type gluons with consistently fixed k_a^2 as input for the BFKL evolution. A further complication is introduced by the necessity to add a background contribution to the BFKL prediction for F_2. Then it seems reasonable to require that the main growth of F_2 be not driven by the chosen background and that this background be comparably small. The last condition is not satisfied in the region of the E665 experiment, casting serious doubts on the good agreement with the data.

In the HERA region, we find in contrast small background contributions, allowing for reliable comparisons with experiment. Especially the preliminary HERA data in Fig. 5 show that the almost Q^2-independent BFKL slope is too steep for $Q^2 \lesssim 15$ GeV^2. But even up to the expected limit of applicability in Q^2 of the BFKL evolution, we find that the predicted slope is somewhat too steep. With improved statistics and maybe a slightly extended coverage in x, HERA should be able to assess the LO BFKL predictions for F_2. If the tendency visible in the current data is an indication for future developments, we expect the LO BFKL equation to fail the test. It remains to be seen whether extensions of the LO BFKL equation—inclusion of the quark sector, NLO BFKL or theoretically consistent (energy-momentum conservation, etc.) unified evolution equations—can improve the agreement with the data. Our results also indicate that conventional (dynamical) renormalization group evolutions are still the best method for calculating and analyzing F_2.

ACKNOWLEDGMENTS

We are grateful to E. Reya and M. Glück for the helpful guidance and fruitful discussions, and to E. Reya, M. Stratmann, and S. Kretzer for carefully reading the manuscript. We thank P. J. Sutton for making the D_0-type partons available to us. I.B. wishes to thank D. Wegener for granting additional computing time on his workstations. This work has been supported in part by the "Bundesministerium für Bildung, Wissenschaft, Forschung und Technologie," Bonn.

TABLE II. Coefficients defined in (A2) of the parametrization (A1).

	D_0-type	D_--type
A	4.818×10^{-3}	8.07×10^{-4}
B	-2.460×10^{-3}	4.1×10^{-5}
C	7.386×10^{-4}	1.579×10^{-4}
D	3.32×10^{-6}	4.370×10^{-5}
E	-2.23×10^{-1}	-1.89×10^{-1}
F	1.15×10^{-2}	1.86×10^{-2}
G	-5.3×10^{-3}	-1.46×10^{-2}
H	-6.66×10^{-4}	-8.72×10^{-4}
I	6.54×10^{-3}	1.026×10^{-2}
J	5.113×10^{-1}	5.700×10^{-1}
K	7.10×10^{-3}	2.89×10^{-3}
Λ_{QCD}	173.2 MeV	230.4 MeV

APPENDIX: PARAMETRIZATION

It should be convenient to have a simple parametrization of our theoretical results for F_2. The following is a parametrization of the BFKL part only, to which an appropriate background still has to be added.

We use an ansatz of the form

$$F_2^{\mathrm{BFKL}} = \alpha x^{-\lambda} + \beta x + \gamma \,, \tag{A1}$$

which describes all curves shown in Figs. 3–6 well. It is even possible to parametrize *all* pure BFKL results for the D_0-type and D_--type gluons shown in Figs. 5 and 6 by choosing the following Q^2 dependence of the coefficients $[t = \ln(Q^2/\Lambda_{\mathrm{QCD}}^2)]$:

$$\begin{aligned} \alpha(Q^2) &= A + Bt + Ct^2 + Dt^3 \,, \\ \beta(Q^2) &= Et^2 + Ft^3 \,, \\ \gamma(Q^2) &= G + H(Q^2/\mathrm{GeV}^2) + It \,, \\ \lambda(Q^2) &= J + Kt \,. \end{aligned} \tag{A2}$$

The corresponding coefficients are given in Table II. It is interesting to note that a small growth of λ with Q^2 has to be taken into account.

It has to be stressed that this parametrization is *only* valid within the range $10^{-5} \leq x \leq 10^{-2}$ and 0.8 GeV^2 $\leq Q^2 \leq$ 120 GeV^2. On the one hand, BFKL evolution is not expected to be applicable even at the edges of this region. On the other hand, we note that the form of the ansatz has been tailored for this region only. The term βx, for example, will lead to wrong results for $x > 10^{-2}$.

[1] G. Altarelli and G. Parisi, Nucl. Phys. **B126**, 298 (1977).
[2] V. N. Gribov and L. N. Lipatov, Yad. Fiz. **15**, 781 (1972) [Sov. J. Nucl. Phys. **15**, 438 (1972)]; **15**, 1218 (1972) [**15**, 675 (1972)]; Yu. L. Dokshitzer, Zh. Eksp. Teor. Fiz. **73**, 1216 (1977) [Sov. Phys. JETP **46**, 641 (1977)].
[3] M. Glück, E. Reya, and A. Vogt, Z. Phys. C **53**, 127 (1992); Phys. Lett. B **306**, 391 (1993).
[4] M. Glück, E. Reya, and M. Stratmann, Nucl. Phys. **B422**, 37 (1994).
[5] M. Glück, E. Reya, and A. Vogt, Z. Phys. C **67**, 433 (1995).
[6] E. A. Kuraev, L. N. Lipatov, and V. Fadin, Zh. Eksp. Teor. Fiz. **72**, 373 (1977) [Sov. Phys. JETP **45**, 199 (1977)]; Ya. Ya. Balitskiĭ and L. N. Lipatov, Yad. Fiz. **28**, 1597 (1978) [Sov. J. Nucl. Phys. **28**, 822 (1978)].
[7] C. Corianò and A. R. White, Phys. Rev. Lett. **74**, 4980 (1995).
[8] M. Ciafaloni, Nucl. Phys. **B296**, 49 (1988); S. Catani, F. Fiorani, and G. Marchesini, *ibid.* **B336**, 18 (1990); R. Peschanski and S. Wallon, Phys. Lett. B **349**, 357 (1995).
[9] J. C. Collins and R. K. Ellis, Nucl. Phys. **B360**, 3 (1991).
[10] J. Kwieciński, A. D. Martin, and P. J. Sutton, Phys. Rev. D **52**, 1445 (1995).
[11] A. J. Askew, J. Kwieciński, A. D. Martin, and P. J. Sutton, Mod. Phys. Lett. A **8**, 3813 (1993).
[12] A. J. Askew, J. Kwieciński, A. D. Martin, and P. J. Sutton, Phys. Rev. D **49**, 4402 (1994).
[13] E665 Collaboration, A. V. Kotwal, in the XXXth Rencontres de Moriond, 1995, edited by J. Tran Thanh Van (unpublished).
[14] H1 Collaboration, T. Ahmed *et al.*, Nucl. Phys. **B439**, 471 (1995); ZEUS Collaboration, M. Derrick *et al.*, Z. Phys. C **65**, 379 (1995).
[15] H1 Collaboration, J. Dainton and G. Rädel, talk given at the Workshop on Deep Inelastic Scattering and QCD, Paris, 1995 (unpublished); ZEUS Collaboration, B. Foster and M. Lancaster, *ibid.*
[16] M. Glück, E. Reya, and A. Vogt, Z. Phys. C **48**, 471 (1990).
[17] A. D. Martin, W. J. Stirling, and R. G. Roberts, Phys. Lett. B **354**, 155 (1995).
[18] A. J. Askew, J. Kwieciński, A. D. Martin, and P. J. Sutton, Phys. Rev. D **47**, 3775 (1993).
[19] J. Kwieciński, Z. Phys. C **29**, 561 (1985).
[20] A. Donnachie and P. V. Landshoff, Phys. Lett. B **296**, 227 (1992).
[21] S. Catani, M. Ciafaloni, and F. Hautmann, Nucl. Phys. **B366**, 657 (1991); S. Catani and F. Hautmann *ibid.* **B427**, 475 (1994).
[22] D. Strozik-Kotlorz, Z. Phys. C **53**, 493 (1992).
[23] H1 Collaboration, S. Aid *et al.*, Phys. Lett. B **354**, 494 (1995).
[24] A. D. Martin, W. J. Stirling, and R. G. Roberts, Phys. Rev. D **47**, 867 (1993).
[25] P. J. Sutton (private communication).
[26] B. Badełek and J. Kwieciński, Phys. Lett. B **295**, 263 (1992).
[27] A. D. Martin, W. J. Stirling, and R. G. Roberts, Phys. Rev. D **51**, 4756 (1995).